

# An extension of Nyquist feedback stability for linear time-varying, discrete-time systems

PRZEMYSŁAW ORLOWSKI  
Institute of Control Engineering  
Szczecin University of Technology  
Sikorskiego 37, 70-313 Szczecin  
POLAND  
orz@ps.pl <http://www.orz@ps.pl>

**Abstract:** The paper concerns on extending the classical Nyquist theorem to stability analysis of linear time-varying (LTV) discrete-time (DT) feedback control systems. Frequency methods, are well-known tool for analysis and synthesis for linear time-invariant systems. Unfortunately, the methods cannot be applied for LTV systems. The main objective is to show that Bode plots approximated using SVD-DFT are adequate methods for evaluating stability margins as well as external stability for LTV systems. We assume discrete-time state space models with time dependent system matrices defined on a finite time horizon. To solve the problem we employ discrete Fourier transform and singular value decomposition of a system matrix operator as well as properties of power spectral density.

**Key-Words:** - discrete-time systems, time-varying systems, non-stationary systems, stability, finite time horizon, frequency analysis

## 1. INTRODUCTION

Classical frequency methods are applicable only to a narrow class of the dynamical systems: linear time invariant (LTI) systems. It refers to all known methods, including the Nyquist stability theorem and measures such as stability margins including the gain margin and phase margin.

Stability of an linear time-varying (LTV) system without feedback was considered in e.g. [1], [2], [3], [4], [5]. The problems are slightly different than for LTI systems. It is well-known that unforced piecewise constant linear systems, whose associated matrix of dynamics takes values in a set of strictly Hurwitzian matrices, are not guaranteed to be exponentially stable [6], [7], [8], [9]. Instability can occur when an infinite number of switches between elements of that set are performed. A surprising result is that time-varying systems with constant and strictly stable eigenvalues may be unstable if the parameters of the dynamics matrix do not vary at a sufficiently small slope [10], [9]. The problem of switching operations between configurations of piecewise continuous stable

dynamics is of growing interest in multimodel design with improved transient performances and of relevant interest in adaptive control.

Many methods for control synthesis (especially frequency domain methods) take advantage of closed-loop stability including calculating the measure of relative stability (the stability margin) e.g. the gain and phase margin. The classical approach for LTI systems is based on the transformation to the  $Z$  domain, where  $z = e^{j\omega T_p}$ . The system is externally stable if the open-loop transfer function is a bounded analytic function of  $z$  in the unit circle. Such an approach cannot be used for LTV systems because the  $Z$  transform can be performed for LTI systems only. Although some methods exist for LTI-uncertain systems, it is not possible to apply it to a frequency design approach for LTV systems.

The main aim of the paper is to discuss why the approximated SVD-DFT Bode diagrams, defined in [11], are adequate tools for estimating stability margins (gain, phase) and for examining the feedback stability for linear time varying (LTV) systems. An LTV state space representation is much more powerful than an LTI model. Recently, it has been often used for improving the accuracy of linear methods, especially when the system originally has nonlinear behaviour [12]. Our method is approximate, unlike the exact LTI systems despite the approximate character of SVD-DFT Bode diagrams, especially the phase diagram. Similarly for LTI systems, it is a graphical method for stability analysis in a feedback loop for LTV systems analogous to LTI ones. The proposed method allows calculation of the gain margin as well as the phase margin. The main tools used for estimating stability for LTV systems are singular value decomposition (SVD), discrete Fourier transform (DFT), and an analogue to the classical Nyquist criterion.

## 2. MODEL OF THE SYSTEM

In order to describe the dynamics of time-varying discrete-time systems, one can use difference equations with time-dependent coefficients or a

generalized description employing state equations with time-dependent matrices in following form:

$$\mathbf{x}_p(k+1) = \mathbf{A}(k)\mathbf{x}_p(k) + \mathbf{B}(k)\mathbf{v}_p(k), \quad (2.1)$$

$$\mathbf{y}_p(k) = \mathbf{C}(k)\mathbf{x}_p(k) + \mathbf{D}(k)\mathbf{v}_p(k), \quad \mathbf{x}_p(0) = \mathbf{0}, \quad (2.2)$$

where  $\mathbf{x}_p(k) \in \mathbf{R}^n$  is nominal state,  $\mathbf{v}_p(k) \in \mathbf{R}^m$  is the nominal control,  $\mathbf{y}_p(k) \in \mathbf{R}^p$  is the nominal output and  $\mathbf{A}(k) \in \mathbf{R}^{n \times n}$ ,  $\mathbf{B}(k) \in \mathbf{R}^{n \times m}$ ,  $\mathbf{C}(k) \in \mathbf{R}^{p \times n}$ ,  $\mathbf{D}(k) \in \mathbf{R}^{p \times m}$  are system matrices,  $k \in \{0, \dots, N-1\}$ .

Alternatively, the system model may be described by means of operators. Then equations (2.1-2.2) can be given in the following form

$$\hat{\mathbf{y}} = \hat{\mathbf{C}}\hat{\mathbf{L}}\hat{\mathbf{x}}_0 + (\hat{\mathbf{C}}\hat{\mathbf{L}}\hat{\mathbf{B}} + \hat{\mathbf{D}})\hat{\mathbf{v}} \quad (2.3)$$

In order that the system (2.3) be equivalent to the system (2.1-2.2), operator  $\hat{\mathbf{C}}\hat{\mathbf{L}}\hat{\mathbf{B}} + \hat{\mathbf{D}}$  must be defined in one of the two equivalent notations: either an evolutionary one, where operators are written by means of sums and products [13], or a matrix-based one, where each of the operators can be presented in terms of matrices. In order to analyze the stability of the system, one has to only know the  $\hat{\mathbf{C}}\hat{\mathbf{L}}\hat{\mathbf{B}} + \hat{\mathbf{D}}$  operator which can be expressed with the help of the following operators:

$$\hat{\mathbf{L}} = \begin{bmatrix} \mathbf{0} & \mathbf{0} & \dots & \mathbf{0} & \mathbf{0} \\ \mathbf{I} & \mathbf{0} & \dots & \mathbf{0} & \mathbf{0} \\ \mathbf{A}(1) & \mathbf{I} & \mathbf{0} & \vdots & \vdots \\ \vdots & \ddots & \mathbf{I} & \mathbf{0} & \mathbf{0} \\ \mathbf{A}(N-2) \dots \mathbf{A}(1) & \dots & \mathbf{A}(N-2) & \mathbf{I} & \mathbf{0} \end{bmatrix} \quad (2.4)$$

$$\hat{\mathbf{B}} = \begin{bmatrix} \mathbf{B}(0) & \mathbf{0} & \mathbf{0} \\ \mathbf{0} & \ddots & \mathbf{0} \\ \mathbf{0} & \mathbf{0} & \mathbf{B}(N-1) \end{bmatrix}, \quad \hat{\mathbf{C}} = \begin{bmatrix} \mathbf{C}(0) & \mathbf{0} & \mathbf{0} \\ \mathbf{0} & \ddots & \mathbf{0} \\ \mathbf{0} & \mathbf{0} & \mathbf{C}(N-1) \end{bmatrix} \quad (2.5)$$

Operator  $\hat{\mathbf{D}}$  has a block diagonal form similar to  $\hat{\mathbf{B}}$  and  $\hat{\mathbf{C}}$ . State  $\mathbf{x}_p(\cdot)$ , output  $\mathbf{y}_p(\cdot)$  and input  $\mathbf{v}_p(\cdot)$  have the following notations:

$$\hat{\mathbf{x}} = \begin{bmatrix} \mathbf{x}_p(0) \\ \vdots \\ \mathbf{x}_p(N-1) \end{bmatrix}, \quad \hat{\mathbf{y}} = \begin{bmatrix} \mathbf{y}_p(0) \\ \vdots \\ \mathbf{y}_p(N-1) \end{bmatrix}, \quad \hat{\mathbf{v}} = \begin{bmatrix} \mathbf{v}_p(0) \\ \vdots \\ \mathbf{v}_p(N-1) \end{bmatrix} \quad (2.6)$$

The input-output operator  $\hat{\mathbf{C}}\hat{\mathbf{L}}\hat{\mathbf{B}} + \hat{\mathbf{D}}$  defined by eq. (2.3-2.5) is a compact, Hilbert-Schmidt operator from  $l_2$  into  $l_2$  and actually maps bounded signals  $\mathbf{v}_p(k) \in \mathbf{V} = l_2[0, N]$  into the signals  $\mathbf{y}_p \in \mathbf{Y}$ .

### 3. THE SVD-DFT FREQUENCY DOMAIN APPROXIMATION ALGORITHM

The basis of the classical Nyquist stability approach for an LTI feedback loop control is the frequency domain representation for an open-loop control system. This representation is usually called the

Nyquist diagram and the regeneration theory begun by Nyquist [14]. Consequently, the necessary condition for self-excited vibration is the synchronous appearance of a phase shift and magnification in an open-loop control.

The main problem with the application-similar methodology for LTV is the absence of the appropriate frequency domain representation of the system. We try to show that the SVD-DFT proposed in [11] satisfies the criteria to be sufficient for an approximate evaluation of feedback stability, gain, and phase margins. A detailed description of the SVD-DFT method is presented in [11]. Here, we only describe the key points.

Frequency responses for LTV systems can be derived using following power spectral density property

$$S_y(\omega_k) = |G(\omega_k)|^2 S_v(\omega_k) \quad (3.1)$$

where  $S_y(\omega_k)$ ,  $S_v(\omega_k)$  are output and input spectral densities respectively.

A frequency response  $|G(\omega_k)|$  can be determined in a unique way if input and output spectral densities of the system are known. It can be done by making use of singular value decomposition. SVD decomposes matrix or matrix system operator into corresponding sets of singular values  $\sigma_i$ , singular input vectors  $\mathbf{v}_i$  and singular output vectors  $\mathbf{u}_i$  i.e.  $\mathbf{USV}^T = \hat{\mathbf{C}}\hat{\mathbf{L}}\hat{\mathbf{B}} + \hat{\mathbf{D}}$ , where  $\mathbf{S} = \text{diag}(\sigma_i)$  is a diagonal matrix, and orthonormal matrices  $\mathbf{U}$ ,  $\mathbf{V}$  are composed of column vectors  $\mathbf{u}_i$  and  $\mathbf{v}_i$  respectively.

Discrete power spectral density (PSD) for any orthonormal matrix originated from SVD is equal to 1 if counted as a sum of power spectral densities of individual matrix columns  $\{\mathbf{V} = \{\mathbf{v}_{ij}\}, i, j = 1 \dots N\}$ .

$$S_v(\omega_k) = \frac{1}{N} \sum_{i=1}^N \left| \sum_{n=1}^N v_{ni} e^{-j2\pi(k-1)(n-1)/N} \right|^2 = 1 \quad (3.2)$$

where  $\omega_k = k / (2T_p N)$ ,  $T_p$  – sampling period.

The output power spectral density can be evaluated as a sum of power spectral densities of individual columns of a matrix defined as a product of  $\mathbf{US}$  matrices. This can be written in the following way:

$$S_y(\omega_k) = \frac{1}{N} \sum_{i=1}^N \left| \sum_{n=1}^N u_{ni} \sigma_i e^{-j2\pi(k-1)(n-1)/N} \right|^2 \quad (3.3)$$

where  $\sigma_i$  –  $i$ th singular value of  $\mathbf{USV}^T = \hat{\mathbf{C}}\hat{\mathbf{L}}\hat{\mathbf{B}} + \hat{\mathbf{D}}$  decomposition.

The main algorithm for the frequency response approximation for LTV discrete-time systems take advantage of the above properties of PSD. Bode diagrams include the magnitude-frequency response  $|G(\omega_k)|$  :

$$|G(\omega_k)| = \sqrt{\frac{1}{N} \sum_{i=1}^N \left| \sigma_i \sum_{n=1}^N u_{ni} e^{-j2\pi(k-1)(n-1)/N} \right|^2} \quad (3.4)$$

which defines it uniquely. Analogously with the latter, the phase-frequency response  $\varphi(\omega_k) = \arg(G(\omega_k))$  can be written as:

$$\varphi(\omega_k) = \arg \left( \sum_{i=1}^N \left( \frac{\sum_{n=1}^N u_{ni} e^{-j2\pi(k-1)(n-1)/N}}{\sum_{n=1}^N v_{ni} e^{-j2\pi(k-1)(n-1)/N}} \right) \right) \quad (3.5)$$

Singular values  $\sigma_i$  in eqs. (3.4-3.5) play their part as weight functions. The derived relationships hold true for both time-invariant and time-variant systems. Characteristics obtained in the way shown for time-invariant systems at a finite time horizon are close to Bode characteristics obtained in the classic way by substituting  $z = \exp(j\omega T_p)$ .

Affinity of the diagrams holds only if a large enough finite time horizon (FTH) is used. The method is only homogeneous but not additive. Approximated Bode diagrams are divided into the magnitude and phase plot. The magnitude  $|G(\omega_k)|$  can be interpreted as a cumulative amplification of all harmonics (output power for unitary input signals) in the output spectra for a given sinusoidal input. While the phase  $\varphi(\omega_k)$  is approximately equal to that of the phase shift of corresponding spectral components in the input and output spectra, taken with appropriate weights given by corresponding singular values. To avoid division-by-zero in eq. (3.5), the terms with the denominator absolute value relatively close to zero, i.e.

$\left| \sum_{n=1}^N v_{ni} e^{-j2\pi(k-1)(n-1)/N} \right| \approx 0$  are omitted in the outer sum (in respect to variable  $i$ ) in eq. (3.5).

#### 4. GENERALIZED LTV SYSTEMS FEEDBACK STABILITY

To employ the classical Nyquist theorem for LTI systems, one must know the number of unstable poles and non-minimal-phase zeros (poles and zeros which lie outside the unitary circle or in the right half plane for continuous systems). In some cases, it is possible to determine the instantaneous values of poles and zeros of the LTV system but in general it is impossible to determine whether the time-varying pole or zero is really stable (minimal-phase). Thus for an LTV system, we cannot determine how many times the point  $-1$  must be encircled. Therefore, the definition below requires stability and a minimal-phase character of the open control loop of the system.

**Theorem 1.** LTV feedback control system is stable when the plant with an open control loop is stable and

the minimal-phase and approximated SVD Nyquist diagram do not encircle the left side the  $-1$  point. Equivalently when the approximated Bode diagrams achieve a  $180^\circ$  phase shift, the open-loop magnification must be less than 1 (0dB).

In other words, the closed-loop LTV system is stable if the magnitude on the Bode diagram is less than 1 (0dB) for a phase shift  $180^\circ \pm k \cdot 360^\circ, k \in Z$ .

The specificity of LTV systems allows one to also generate time-varying vibrations, e.g. shifting between different eigenvectors within a generation. Therefore, the LTV system may generally generate wide frequency spectra (time-varying generation). Moreover, the correlation existing between different spectras can introduce some inaccuracy to results of the proposed method as an insufficiently short time horizon may similarly cause underestimated results.

Adaptation of the classical Nyquist stability criteria for LTV systems needs some justification. First of all, there are important differences between the decomposed LTI and LTV feedback control systems from the input-output point-of-view. The product of the SVD consists of 3 matrices: the input  $\mathbf{V} = [\mathbf{v}_1, \dots, \mathbf{v}_N]$ , transfer diagonal  $\mathbf{S}$ , and the output  $\mathbf{U} = [\mathbf{u}_1, \dots, \mathbf{u}_N]$ . Input and output matrices consist of a column of singular input and output vectors respectively. Let the input of the system be an arbitrary singular vector  $\mathbf{v}_k$ . After passing the plant, it takes the form of  $\mathbf{y} = \mathbf{u}_k \mathbf{s}_k$ . When the plant is controlled in a negative feedback loop, the signal is subtracted from the input. New output of the system depends on the type of the system. For an LTI system, the output signal takes the general form  $A\mathbf{v}_{k,n}$  whereas for a LTV system, it takes the following general form  $A\mathbf{v}_{k,n} + B_1\mathbf{v}_{k1,n1} + B_2\mathbf{v}_{k2,n2} + \dots$  where  $n$  denotes time shifts and  $k$  singular vectors. It is clear that the LTV system not only changes the amplitude and phase of the input signal but also may introduce new associated vectors ( $k1, k2, \dots$ ).

For example, let us assume an open-loop system which magnifies the sinusoidal signal with frequency  $f_0$  slightly smaller than unity with a simultaneous  $180^\circ$  phase shift. Although such an LTI system is stable in the feedback loop, the LTV system need not be stable in the closed control loop. The LTV system allows modulation phenomenon and the main band  $f_0$  may generate side bands with the frequency  $f_1$  in the output spectra. If the system modulation of feedback frequency  $f_1$  induces a band in frequency  $f_0$ , the resultant magnification can be larger than unity and the feedback loop may be unstable, especially in the case of favorable amplifications and phase shifts.

It is obvious that for an LTV system, the main factor of importance for feedback stability of an LTV system

is the apparent magnification following from the analysis of the whole output spectra for a given input signal. Simply measuring the input/output magnification for a given sinusoidal input is insufficient.

The following question arises: how do we obtain the apparent magnification and phase shift of LTV system? Using empirical methods, one can easily measure the main band magnification for input sinusoidal signals with frequencies from the given range. Nevertheless, such data do not take the modulation phenomena into account.

Using the SVD-DFT method, one can approximate the magnitude diagram (3.4) as a weighted quadratic mean of the DFT magnitude for singular vectors of the system operator. The phase diagram (3.5) can be approximated as a weighted mean of DFT shifts for singular vectors of the system operator. Described above are square-averaged diagrams that took typical phenomena into account for LTV systems such as modulation, frequency transitions etc.

It should be emphasized that for such diagrams, the system may be border line stable for conditions analogous to LTI systems (gain 1, phase shift 180°). It is caused not only by numerical reasons (finite time horizon, limited resolution in time domain, etc.) but also by undetermined transitions between different frequencies. The SVD-DFT method uses the power spectral density which represents the worst case of transitions in the spectra. Magnification on the diagram (3.4) can be understood as the square root of the output signal power for a sinusoidal input with unity power. Thus, the real critical gain is always less than or equal to the corresponding value read out from approximated SVD-DFT Bode diagrams. In many cases, the values are quite close, especially for weak LTV systems (slowly varying and/or insignificant variations) [11], [15].

## 5. NUMERICAL EXAMPLE

We consider a planar robotic manipulator with varying inertia links is used as a LTV system and shown in Fig. 5.1. The manipulator is placed in a horizontal plan and each link has sliding mass  $\mu_i$  whose position  $r_i(t)$  can be varied. Such a manipulator was discussed in [16], [1] and the idea of the use of inertia links is to compensate external perturbation by varying the position of the sliding masses. To model the system, the following assumptions are used. The links are uniform rigid bars of equal length  $l$  and mass  $m$ . The first link is connected to the base by means of an elastic spring-hinge of rotational stiffness  $k_1$ . The second link is connected to the first link by a similar spring of stiffness  $k_2$ . The viscous damping is modeled by the rotary dampers  $d_1$  and  $d_2$ . The angles  $\varphi_1$  and  $\varphi_2$

denote the angular positions of the links relative to the x-axis. When disturbed, the links vibrate about their equilibrium positions  $\varphi_{10}$  and  $\varphi_{20}$ . The actual angular positions of the links become  $\varphi_1 = \varphi_{10} + \varphi_{11}$  and  $\varphi_2 = \varphi_{20} + \varphi_{21}$ . With the assumption of small angular vibrations, a linearized model for the system is defined by a matrix equation

$$\mathbf{M}(t)\ddot{\boldsymbol{\varphi}}(t) + \mathbf{D}(t)\dot{\boldsymbol{\varphi}}(t) + \mathbf{K}\boldsymbol{\varphi}(t) = \mathbf{q}(t) \quad (5.1)$$

$$\mathbf{M}(t) = \begin{bmatrix} a_1 + \mu_2 l^2 + \mu_1 r_1^2 & (a_2 + \mu_2 l r_2) \cos(\Delta\varphi_0) \\ (a_2 + \mu_2 l r_2) \cos(\Delta\varphi_0) & a_3 + \mu_2 r_2^2 \end{bmatrix} \quad (5.2)$$

$$\mathbf{D}(t) = \begin{bmatrix} d_1 + d_2 + 2\mu_1 r_1 \dot{r}_1 & -d_2 + \mu_2 l \dot{r}_2 \cos(\Delta\varphi_0) \\ -d_2 + \mu_2 l \dot{r}_2 \cos(\Delta\varphi_0) & d_2 + 2\mu_2 r_2 \dot{r}_2 \end{bmatrix} \quad (5.3)$$

$$\mathbf{K} = \begin{bmatrix} k_1 + k_2 & -k_2 \\ -k_2 & k_2 \end{bmatrix}, \quad \boldsymbol{\varphi}(t) = [\varphi_{11} \quad \varphi_{21}]^T \quad (5.4)$$

$$a_1 = \frac{3}{4} m l^2, \quad a_2 = \frac{1}{2} m l^2, \quad a_3 = \frac{1}{3} m l^2, \quad \Delta\varphi_0 = \varphi_{10} - \varphi_{20} \quad (5.5)$$

In the simulation, the following numerical quantities were used: the length  $l=1\text{m}$ , the mass  $m=2\text{kg}$ , the sliding masses  $\mu_1=\mu_2=0.5\text{kg}$ , the stiffness  $k_1=100\text{Nm/rad}$ ,  $k_2=80\text{Nm/rad}$ , and the damping coefficients  $d_1=0.5\text{Nm/rad/s}$ ,  $d_2=0.4\text{Nm/rad/s}$ . The configuration of the manipulator is  $\Delta\varphi_0=45^\circ$ . The model has been adopted directly from [1].

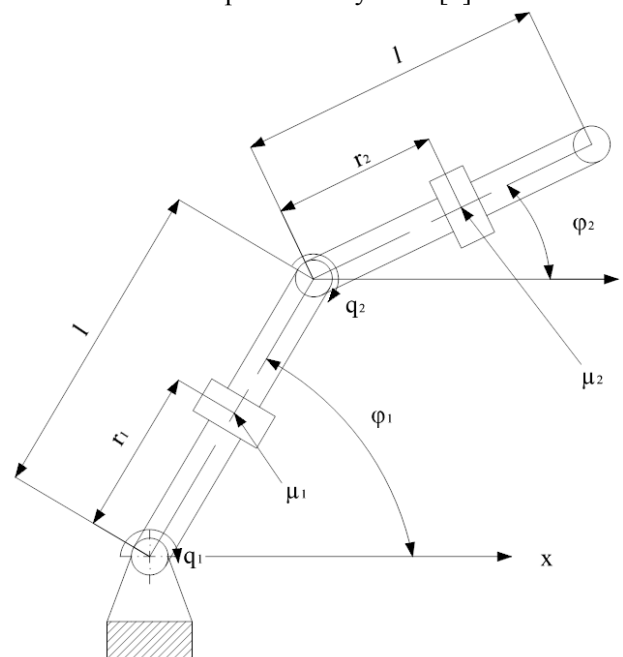


Fig. 5.1. Robotic manipulator with varying inertia links.

To employ the SVD-DFT method, the continuous-time model is discretized using zero order hold on the inputs and period  $T_p=0.005$  s. Analysis is carried out for simplified SISO system with input  $q_1$  and output  $\dot{\varphi}_1$ . The system is 4<sup>th</sup> order with an assumed time

horizon of  $N=1000$  steps. The eigenvalues' positions in the simulation horizon are depicted in fig. 5.2.

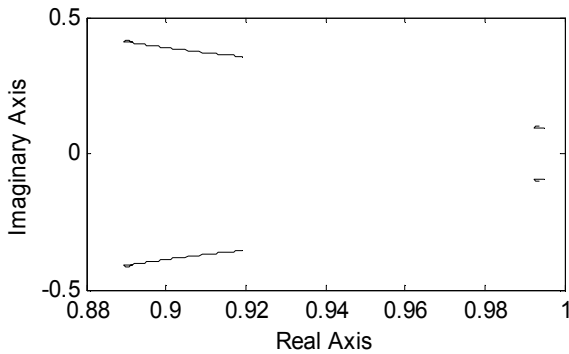


Fig. 5.2. Location of eigenvalues of matrix  $\mathbf{A}(k)$  for a robotic manipulator system  $N=1000$ .

In order to test properties of the proposed stability method, it is reasonable to analyse their behaviour in the case when the system is critically stable. To perform this test, we need amplifications corresponding to phase shift of  $\pm 180 \pm m \cdot 360$  deg on the amplitude diagram. Approximated Bode diagrams are depicted in fig. 5.3 and for the open control loop impulse response on fig. 5.4.

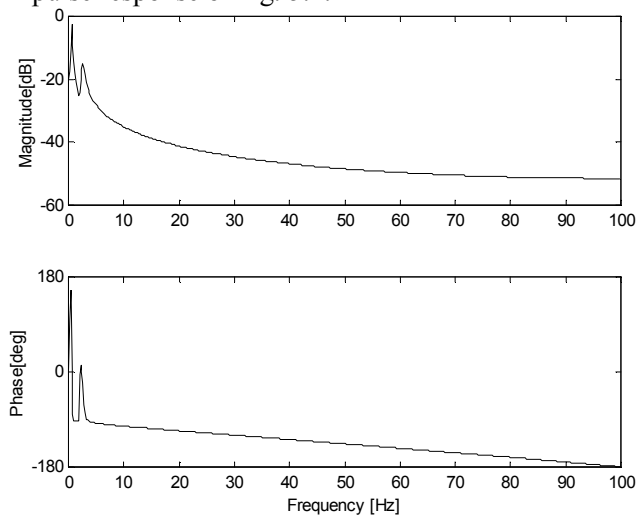


Fig. 5.3. Approximated SVD-DFT Bode plots determined for  $N=1000$ .

An alternative for approximated 2D diagrams from fig. 5.3 are transformed using DFT 3D shifted impulse responses. Such responses can be easily computed by column DFT transform of system operator  $\hat{\mathbf{C}}\hat{\mathbf{L}}\hat{\mathbf{B}} + \hat{\mathbf{D}}$ . Magnitude and phase 3D diagrams are shown on fig. 5.5-6. Nevertheless the diagrams are much more difficult to analyze.

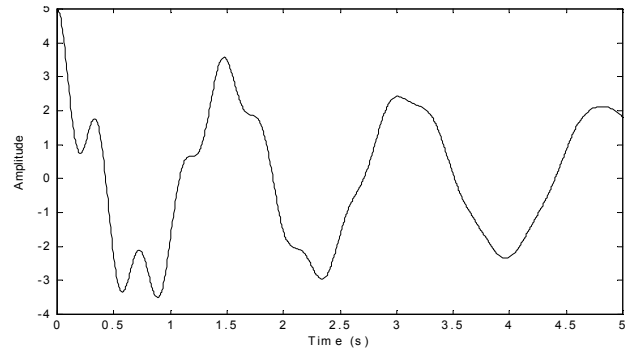


Fig. 5.4. Impulse responses for a robotic manipulator system with open control loop  $N=1000$ .

Eigenfrequencies read from fig. 5.3 are 0.6 Hz and 2.6 Hz. Comparing this to the PMP analysis, Liu [1] (case 1) has computed that eigenpulsations were included in the sets  $\omega_{d1} \in (3.64, 4.15)$ ,  $\omega_{d2} \in (-14.75, 17.5)$  rad/s and corresponding pseudo-damping rates were included in  $\delta_1 \in (-0.11, -0.03)$  with a time average of  $\delta_{a1} = -0.3$  and  $\delta_2 \in (-0.8, -0.55)$  and  $\delta_{a2} = -0.7$ . Converting frequency in radians to Hertz using the equation  $f = \omega / 2\pi$ , the results for both methods are almost the same.

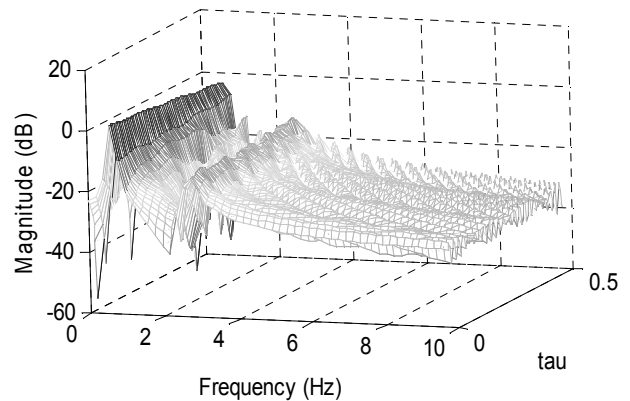


Fig. 5.5. Magnitude 3D plot for transformed impulse responses vs. frequency and time shift ( $\tau$ )  $N=200$ .

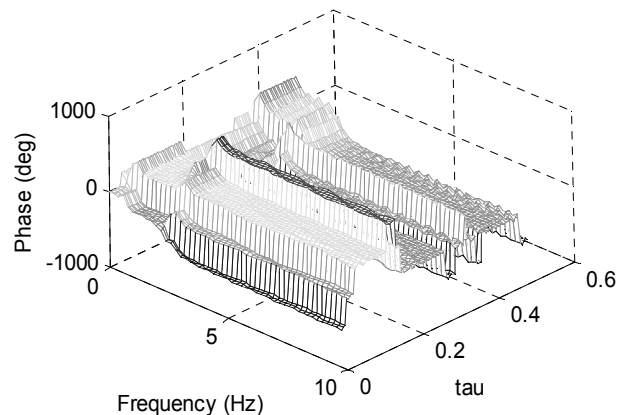


Fig. 5.6. Phase 3D plot for transformed impulse responses vs. frequency and time shift ( $\tau$ )  $N=200$ .

The system is stable so the critical gain can be found for the closed control loop. From fig. 5.3, it can be seen that for  $f=100$  Hz,  $\arg(G(100))=180^\circ$  and  $m_{dB} = |G(100)| = -51.45$  dB. Thus, the system has a stability margin and a gain margin equal to 51.45 dB. The critical gain found experimentally is close to  $m_{dB}=51.45$  dB and equal to  $k_{crit\_dB} = 52$  dB. Fig. 5.7 shows 5 impulse responses for a system with feedback: one for  $k_{crit}=398$  in the linear scale and 4 for gains  $k$  which differ from  $k_{crit}$  by  $\pm 1\%$  and  $\pm 2\%$ .

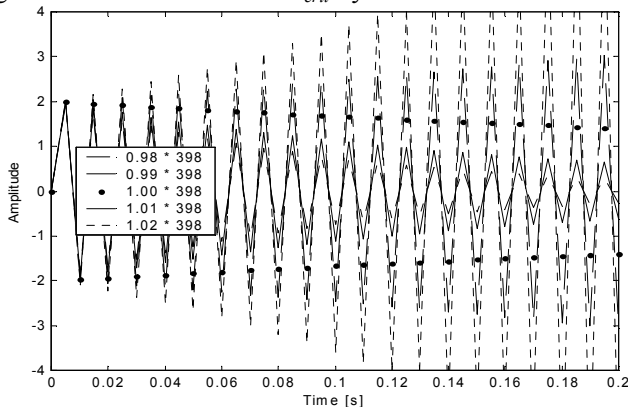


Fig. 5.7. Impulse responses for a robotic manipulator system with feedback loop and proportional controller  $N=40$ .

## 6. CONCLUSION

The paper has shown that the concept of frequency diagrams for discrete-time LTV systems defined on FTH can be used for feedback stability analysis and to estimate relative stability measures – amplitude and phase margins. Moreover the well-defined Nyquist stability criterion may be extended for LTV systems. The SVD-DFT method for LTV systems preserves certain properties of conventional frequency analysis tools for LTI systems. It makes it possible to take advantage of the classical frequency-based approach defined for LTI systems and apply it almost directly to the LTV case.

An important achievement of this work is the generalization of the well-known Nyquist stability theorem for LTV systems using the SVD-DFT method. Although the results for LTV systems are only approximated (close to true), it is now possible to determine the amplitude and phase margin as well as the critical amplification gain for a closed control loop of an LTV system.

## REFERENCES

[1] K. Liu. *Extension of modal analysis to linear time-varying systems*. Journal of Sound and Vibration **226**, 149-167, 1999.

- [2] S. Shokoohi, L. Silverman. *Linear time-variant systems: stability of reduced models*. Automatica, Vol. 20, pp. 59-67, 1987.
- [3] D. O. Anderson, *Internal and external stability of linear time varying systems*. SIAM Journal on Control and Optimization, 20:408–413, 1982.
- [4] P. Iglesias. *Input-output stability of sampled-data linear time-varying systems*. IEEE Trans. Aut. Cont., 40(9):1647-1650, 1995.
- [5] H. S. Han and J. G. Lee, *Necessary and sufficient conditions for stability of time-varying discrete interval matrices*, Int. J. Control, vol. 59, no. 4, pp. 1021–1029, 1994.
- [6] D. E. Miller, E. J. Davison, *An adaptive controller which provides Lyapunov stability*. IEEE Trans. Automat. Control, 34, 599–609, 1989.
- [7] K. S. Narendra, J. Balakrishnan, *Adaptive control using multiple models*. IEEE Trans. Automat. Control, 42, 171–187, 1989.
- [8] R. N. Shorten, K. S. Narendra, *On the stability and existence of common Lyapunov functions for stable linear switching systems*, Proc. of the 37th IEEE Conference on Decision and Control. Tampa, FL, pp. 3723–3724, 1998.
- [9] M. De La Sen, *Robust stability of a class of linear time-varying systems*, IMA Journal of Mathematical Control and Information 19, 399-418, 2002.
- [10] H. K. Khalil, *Nonlinear Systems (Second Edition)*. Englewood Cliffs, NJ: Prentice-Hall, 1996.
- [11] P. Orłowski. *Selected problems of frequency analysis for time-varying discrete-time systems using singular value decomposition and discrete Fourier transform*. Journal of Sound and Vibration, Vol. 278, pp. 903-921, 2004.
- [12] Dutka, A., Ordys A., *The Optimal Non-linear Generalised Predictive Control by the Time-Varying Approximation*, Proc. of 10th IEEE Int. Conf. MMAR. Międzyzdroje. Poland. pp. 299-304, 2004.
- [13] P. Orłowski, *Applications of Discrete Evolution Operators in Time-Varying Systems*. European Control Conference, Porto, pp. 3259-3264, 2001.
- [14] H. Nyquist, *Regeneration theory*, Bell Laboratories Technical Journal, 11, 126–147, 1932.
- [15] P. Orłowski. *Determining the degree of system variability for time-varying discrete-time systems*. 16th IFAC World Congress, Praha 2005.
- [16] G. Jumarie, *Trajectory control of manipulators with time-varying inertia links*. Robotica, **6**, pp. 197-202, 1988.